Supporting Information

TiO_2/ZnO Nanocomposites with Metal-Free Dye and Polymer Gel Electrolyte: Optimizing Photovoltaic Efficiency and Assessing Stability by Time Series Analysis

Prakash S. Pawar[a,b], Pramod A. Koyale[c], Satyajeet S. Patil[d], Swapnil R. Patil[e], Jinho Bae[e], Nilesh R. Chodankar[f], Yash G. Kapdi[g], Saurabh S. Soni[g], Pramod S. Patil[d,h], Sagar D. Delekar[a,*]

[a]Department of Chemistry, Shivaji University, Kolhapur 416004, Maharashtra, India

[b]Department of Chemistry, Shri. Yashwantrao Patil Science College, Solankur, Kolhapur 416216, Maharashtra, India

[c]School of Nanoscience and Biotechnology, Shivaji University, Kolhapur 416004, Maharashtra, India

[d]Thin Film Materials Laboratory, Department of Physics, Shivaji University, Kolhapur 416004, Maharashtra, India

[e]Department of Ocean System Engineering, Jeju National University, 102 Jejudaehakro, Jeju 63243, Republic of Korea.

[f]Mechanical Engineering Department, Khalifa University of Science and Technology, Abu Dhabi 127788, United Arab Emirates

[g]Department of Chemistry, Sardar Patel University, Vallabh Vidyanagar, Anand, Gujarat 388120, India

[h]Honorary University Chair Professor, National Dong Hwa University, Hualien, 974301, Taiwan

***Corresponding Author:** Prof. Sagar D. Delekar (sdd_chem@unishivaji.ac.in)

Experimental Section

Synthesis of TiO_2 nanoparticles (NPs)

TiO_2 NPs were synthesized via sonochemical assisted sol-gel technique, which was reported previously by our research group[1]. Initially, titanium tetraisoproxide [Ti (OCH $(CH_3)_2)_4$] (IV) was added to glacial acetic acid with constant stirring to form a clear solution. To avoid the agglomeration, sodium dodecyl sulfide ($NaC_{12}H_{25}SO_4$) was added to the above clear solution followed by the addition of 100 mL distilled water (DW) with constant stirring for 3 hrs. at 60^{o}C. Thereafter, a dilute solution of sodium hydroxide (NaOH) was added for complete hydroxylation to form titanium hydroxide [Ti $(OH)_2$]. The above solution of Ti $(OH)_2$ was heated to 60^{o}C with constant stirring for 3 hrs. Afterward, the solution was cooled and centrifuged followed by washing with DW. The final white-colored powder of TiO_2 NPs was obtained after calcination at 450^{o}C for 2 hrs.

Synthesis of ZnO nanorods (NRs)

ZnO NRs were prepared by using zinc nitrate as precursors [Zn $(NO_3)_2$].6H_2O, as per the above synthetic route of TiO_2 NPs.

Characterization Tool

Optical properties were studied using UV-visible diffuse reflectance spectra (DRS) through a UV-visible spectrophotometer (LABINDIA, UV 3092) and photoluminance spectra (PL) analysis through a PL spectrophotometer (Jasco Spectrofluorometer, FP-8300). The x-ray diffraction (XRD) (Bruker, AXS D8 Advance) equipped with a Cu Kα target having a wavelength (λ) of 1.5046 ^{0}A and diffraction angle (2θ) ranged from 10° to 80°. X-ray photoelectron spectroscopy (XPS) analysis was recorded at 1.0×10^{-9} Torr base pressure with a monochromatic Al-Kα X-ray source (ESCALAB 250XI, Thermo Fisher Scientific). The surface morphology and elemental compositions were assessed using a scanning electron microscope with a built-in energy dispersive X-ray spectroscopy (EDX) testing facility (MIRA-3 TESCON FESEM). High-resolution transmission electron microscopy (HR-TEM) images and EDX mapping were captured utilizing the TEM (Talos F200X G2) housed at Jeju National University. To prepare the sample for HR-TEM analysis, a minor quantity of the TZ-3 NCs powders was dispersed in ethanol, followed by 15 min of bath sonication. Subsequently, the resulting dispersions were dropcasted onto a 3 mm carbon film-coated Cu grid with a mesh size of 200 (SPI). Surface area and pore size analysis were executed using a Brunauer–Emmett–Teller (BET) surface analyzer (Quantachrome NOVA1000e, USA).

Further, I–V measurements of the device were carried out using a Keithley2400sourcemeter and solar simulator (PET, USA) with a 100Wxenon lamp as a light source equipped with a band pass filter, and light intensity was set to 100 mW/cm^2 (Si-photodiode standard were used to calibrate the light intensity) with one sun illumination were employed to knowing the light to electricity conversion efficiency.

Result and Discussion

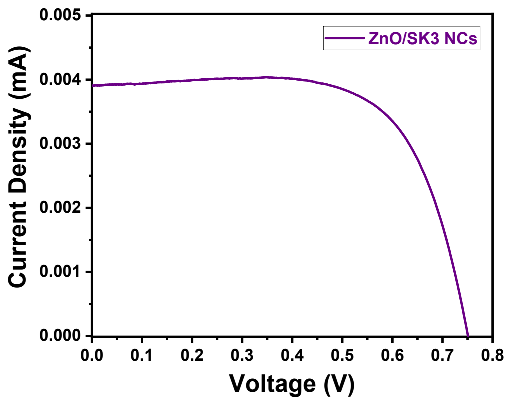

Figure S1. I-V curve for ZnO/SK3-based DSSCs under AM 1.5G sunlight condition.

Table S1. The statistical data of photovoltaic performance

Sample	J_{SC} (mA.cm^{-2})	V_{OC} (V)	I_{MP} (mA.cm^{-2})	V_{MP} (V)	FF (%)	η (%)
TiO_2/SK3	4.07 ± 0.1	0.94 ± 0.02	2.91 ± 0.09	0.82 ± 0.02	62.37	2.38 ± 0.04
ZnO/SK3	3.90 ± 0.07	0.75 ± 0.03	3.56 ± 0.07	0.56 ± 0.02	68.15	1.99 ± 0.02
TZ-1/ SK3	5.72 ± 0.08	0.80 ± 0.01	4.94 ± 0.08	0.68 ± 0.01	73.40	3.05 ± 0.03
TZ-3/ SK3	7.17 ± 0.04	0.89 ± 0.01	6.49 ± 0.05	0.66 ± 0.01	67.12	4.30 ± 0.01
TZ-5/ SK3	6.49 ± 0.09	0.93 ± 0.02	5.53 ± 0.08	0.72 ± 0.01	65.96	3.98 ± 0.02

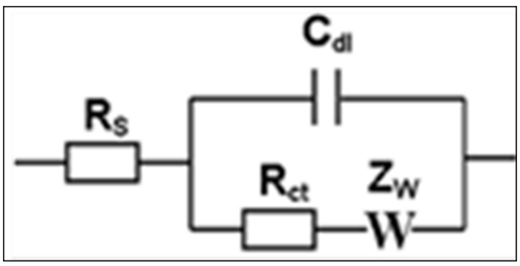

Figure S2. Equivalent circuit model by EIS analysis.

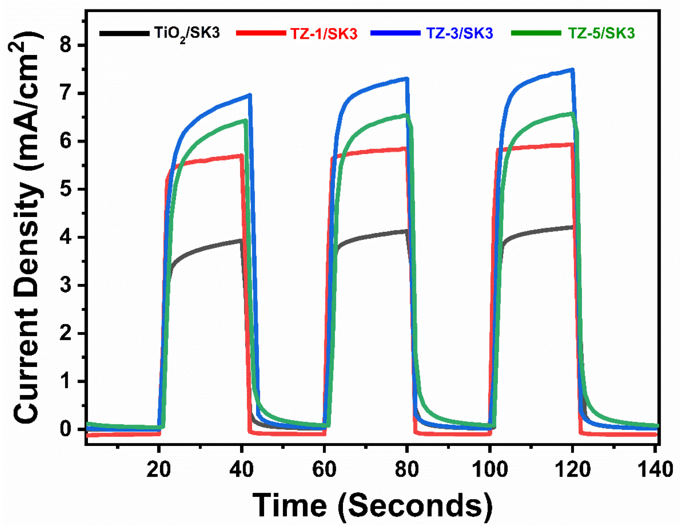

Figure S3. Chronoamperometric stability for designed photoanodes.

Figure S4 (a) shows UV-visible DRS spectra and band gap energy of synthesized bare TiO_2 NPs, TZ-1, TZ-3, and TZ-5 NCs samples recorded in the wavelength region of 200 -800 nm. All samples were recorded, absorption in UV region as well as visible region appearance with high transparency. From the UV-DRS spectra, TiO_2 NPs show an absorption peak of 374.01 nm, due to the electron transfer from the valence to the conduction band (i.e. band to band transition)[2]. Accordingly, the absorption of NCs slightly shifted towards a red shift with increasing the concentration of ZnO in TiO_2 NPs (i.e. TZ-1, TZ-3, and TZ-5) may be due to the synergistic impact. Further, the band gap energy was calculated by using Tauc plots of synthesized TiO2 NPs observed at 3.21 eV. Further, the band gap energy of TZ-1, TZ-3, and TZ-5 NCs corresponds to 3.17 eV, 3.13 eV, and 3.06 eV respectively, which confirms the addition of ZnO content into TiO_2 NPs, band gap energy becomes slightly decreased and shown in **Figure S4 (b).** Due to the increase in light absorption intensity in TiO2-ZnO NCs also it may due to the combined effect of Eg of anatase TiO_2 (3.20 eV) and ZnO (3.3 eV). Furthermore, ZnO may also serve as a constituent in TZ-1, TZ-3, and TZ-5 NCs. Also, the interfacial coupling effect between TiO_2 and ZnO NPs can cause the red shift in the band gap[3,4].

The photoluminance (PL) technique is an essential tool to study the electron-hole pair recombination process occurring in a semiconductor. The low PL intensity reveals the low recombination of electron-hole pairs. The PL spectra of synthesized TiO_2 NPs and TZ-3 (7:3 molar ratios) NCs were indicated in **Figure S4 (c).** The excitation wavelength of synthesised TiO2 NPs is 361.64 nm as well as TZ-3 NCs 370.35 nm. Furthermore, the emission peaks of the bare TiO_2 NPs and TZ-3 NCs observed at NPs are 411.70 nm and 415.99 nm corresponding to 3.011 eV and 2.98 eV[5]**.** Also, the PL intensity of bare TiO_2 NPs is higher as well as higher recombination of photo-excited electrons and holes than the TZ-3 NCs. Due to the different favorable redox energy levels of the valence band and conduction band of the TiO_2 and ZnO, this leads to the effective interfacial charge transfer process and thereby minimizes the electron and hole recombination process[6]. Herein, PL analysis does not show a noticeable difference between bare TiO_2 and TZ-3 NCs, since the content of ZnO NRs with TiO_2 lattice in TZ-3 NCs is less compared to host materials, affecting less PL spectrum of NCs which might also show comparable recombination rate. As well as the decreased PL intensity after the engineering of the TiO_2 lattice revealed reductions in the radiative recombination of photoinduced electrons trapped at the surface of TiO_2 with the content of ZnO NPs, so the said NCs exhibited efficient charge separation as well as transportation[7].

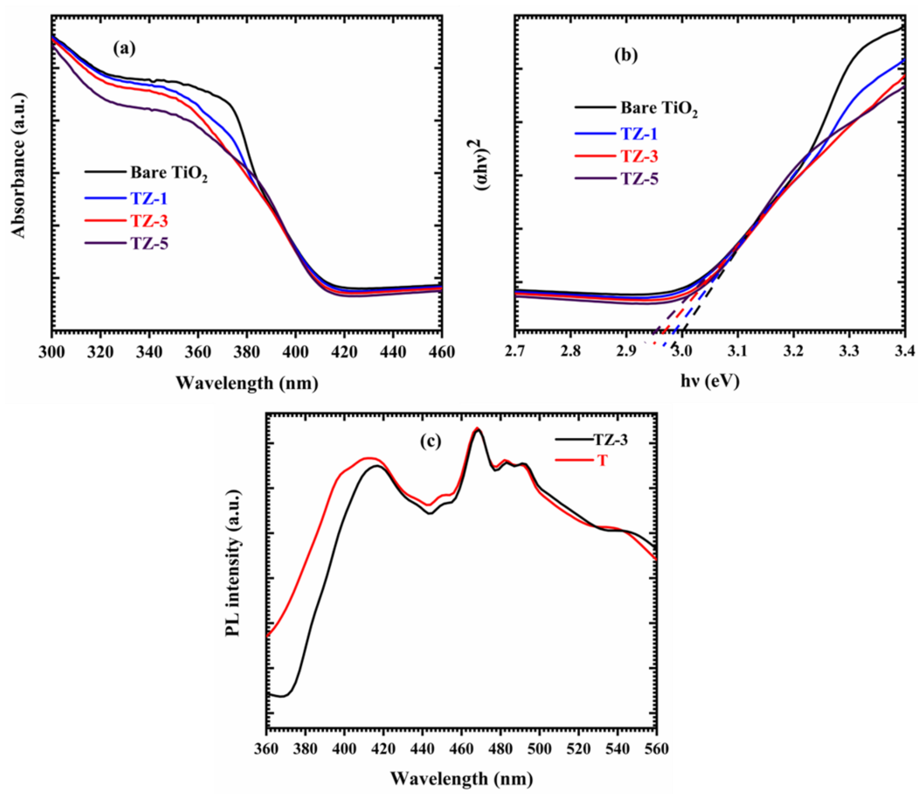

Figure S4. a) UV-visible diffuse reflectance spectroscopy (absorption mode), b) Tauc plot $(\alpha h\nu)^2$ versus photon energy ($h\nu$) with varying content ZnO NPs in TZ NCs, c) PL Spectra of synthesized TZ-3 NCs, and TiO_2 NPs.

Table S2. Calculated bandgap values of synthesized TiO_2 NPs, TZ-1, TZ-3, and TZ-5 NCs as a photoanode form Tauc plots

Sample	Band gap (eV)
TiO_2 NPs	**3.21**
TZ-1 NCs	**3.17**
TZ-3 NCs	**3.13**
TZ-5 NCs	**3.06**

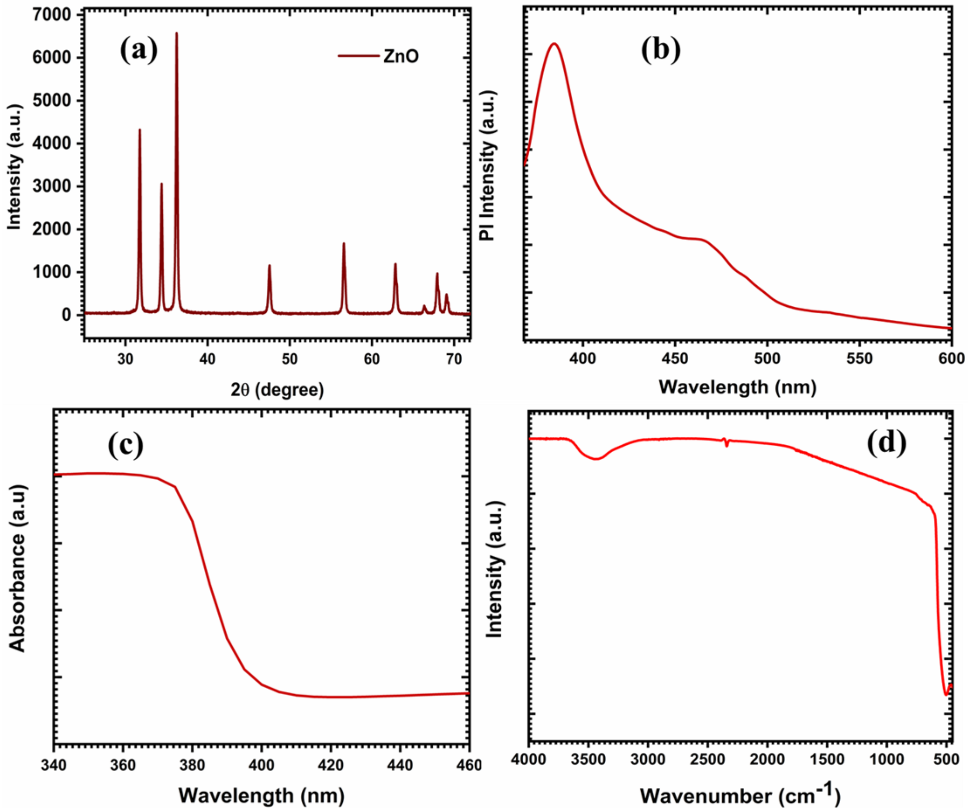

Figure S5. a) XRD, b) photoluminance analysis, c) UV-visible DRS, and d) FT-IR analysis of bare ZnO NRs.

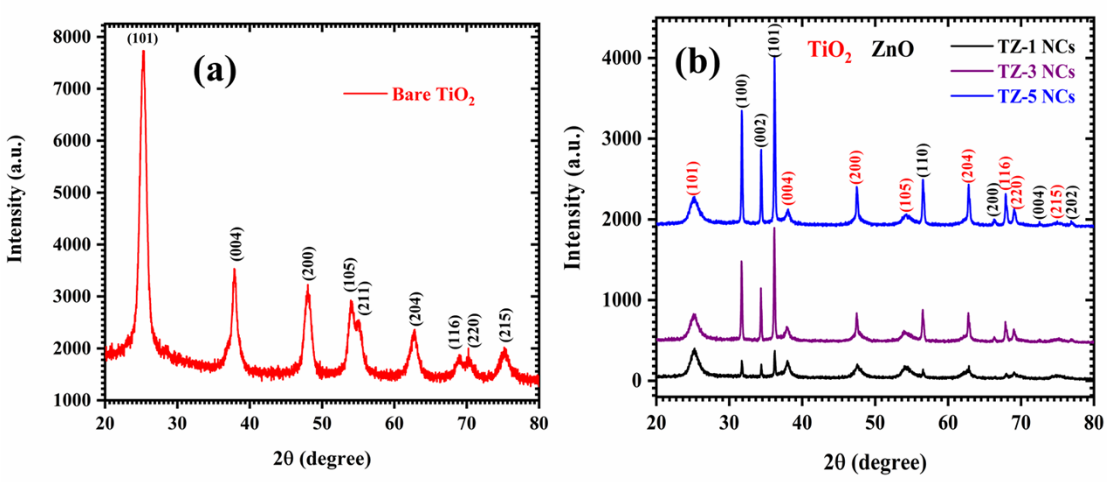

Figure S6. XRD pattern of synthesized a) TiO_2 NPs, b) TZ-1, TZ-3 and TZ-5 NCs.

FT-IR spectra have been performed to demonstrate the functional group and M-O bond presence in synthesized TiO_2 NPs and TZ-3 NCs samples were recorded in wave number range from 4000 to 400 cm^{-1} and shown in **Figure S7.** The peak position at 468.94 cm^{-1} to 797.26 cm^{-1} assigned to the symmetric stretching frequency of O-Ti-O, Ti-O-Ti, Zn-O-Ti, and Zn-O flexion vibrations respectively[8]**.** Among the peak intensity at 683.99 cm^{-1}, this bond vibration confirmed the proper interconnectivity within the TZ-3 NCs. Furthermore, the peak position obtained at 1630.36 cm^{-1} is related to the M-OH (i.e Ti-OH) and C=O stretching of titanium tetraisopropide as a precursor while the peak position observed at 1072.22 cm^{-1} belongs to the M-O-C functional moiety (i.e Ti-O-C or Zn-O-C)[8]. The wide peak position obtained at 3423.80 cm-1 indicates the presence of stretching frequency of the free hydroxyl (–OH) group and also 2928.04 to 2844.02 cm^{-1} is due to the presence of symmetric and asymmetric stretching frequency of $–CH_2$ group and C-O stretching frequncy[9].

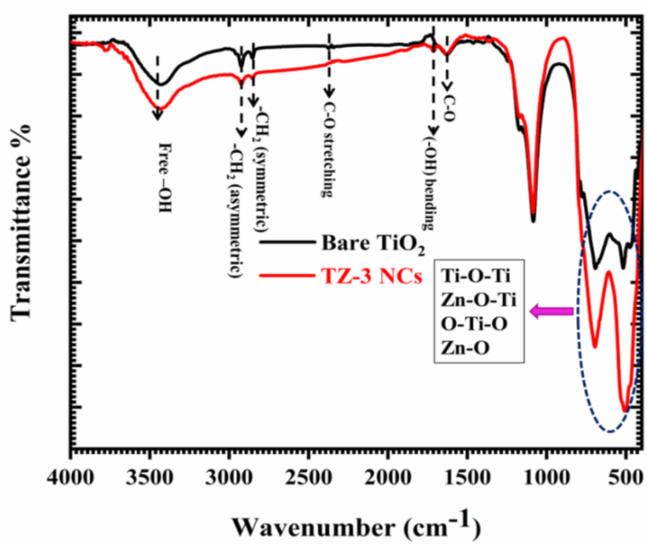

Figure S7. FT-IR spectra of synthesized TiO_2 NPs and TZ-3 NCs.

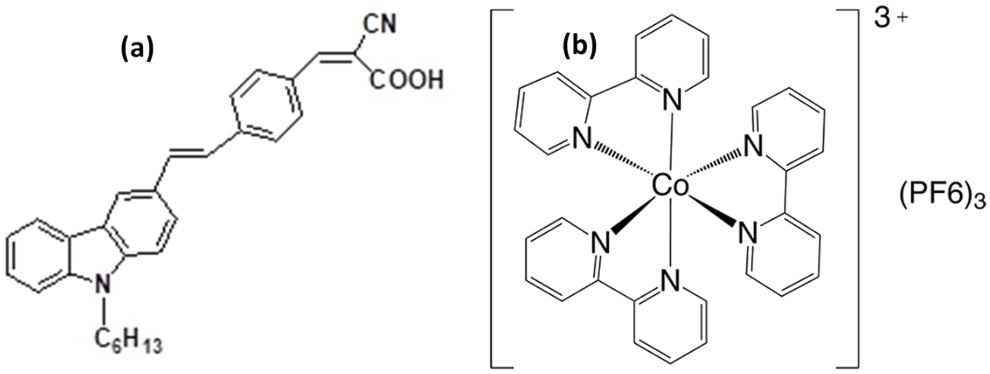

Figure S8. a) Structure of SK3 dye, and b) structure of redox electrolyte.

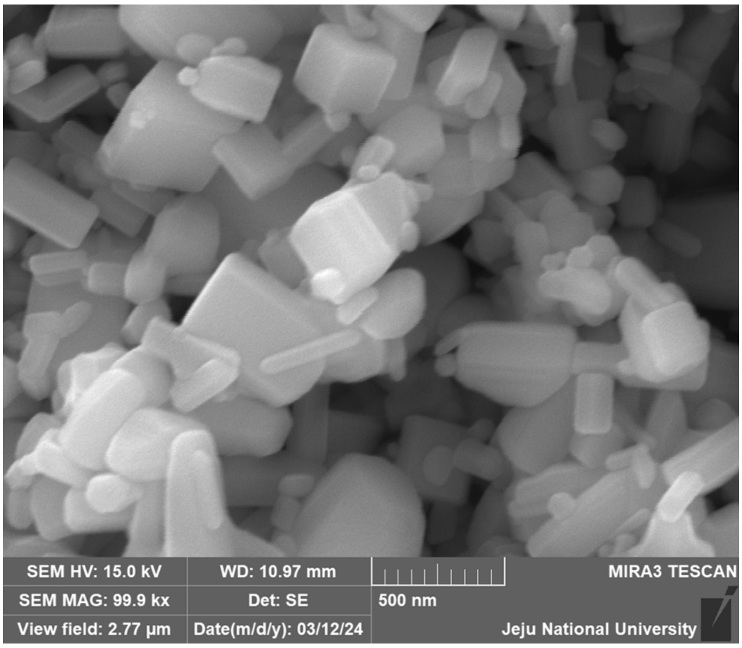

Figure S9. FE-SEM image of bare ZnO.

Table S3: Comparison of the present study with previously reported TiO_2-based photoanode

Material	Synthesis route	Electrolyte	Photovoltaic Parameters				Ref.
			J_{SC}	V_{OC}	FF	η	
TiO_2/ZnO NCs	Simple combined hydrolysis and refluxing method	I_3^-/I^-	2.56	0.63	57	0.91	[3]
TiO_2/ ZnO core-shell	Drop casting method	I_3^-/I^-	2.1	0.54	49	0.55	[3]
TiO_2/ZnO core-shell	sol-gel–reflux method	Oxide-dye-electrolyte interface	1.33	0.606	58.8	0.53	[10]
TiO_2/ZnO NCs	Two-step sol-gel and hydrothermal method	Liquid electrolyte	1.60	0.59	59.4	0.56	[11]
ZnO/ TiO_2 core-shell	Combination of chemical growth and direct current (DC) magnetron sputtering (MS) method.	Liquid electrolyte	1.792	0.665	31	0.35	[12]
TiO_2/ ZnO NCs	Sol-gel processes	PEO–PVDF-HFP-MMT	3.3	0.65	77	1.6	[13]
TiO_2 NP/ZnO nanofiber	Electro spinning and calcination	(I^-/I_3^-)	12.83	0.764	66.69	6.54	[14]
ZnO/CuO NCs	Co-precipitation route	I_3^-/I^-	6.17	0.67	0.63	2.57	[15]
TiO_2/ZnO NCs	Ex-situ sol-gel method	Co^{2+}/Co^{3+}-based PEO–PEG polymer gel	7.17	0.89	67.12	4.30	**Present report**

References

1. Pawar, P. S. *et al.* Optimized Nb-Doped TiO_2/rGO Nanocomposites for Assessment of Photovoltaic Performance With Metal-Free Dye and Polymer Gel Electrolyte. *ChemistrySelect* **9**, e202402098 (2024).

2. Zhao, Y. *et al.* Zn-doped TiO_2 nanoparticles with high photocatalytic activity synthesized by hydrogen–oxygen diffusion flame. *Appl. Catal. B Environ.* **79**, 208–215 (2008).

3. Manikandan, V. S., Palai, A. K., Mohanty, S. & Nayak, S. K. Eosin-Y sensitized core-shell TiO_2-ZnO nano-structured photoanodes for dye-sensitized solar cell applications.

J. Photochem. Photobiol. B Biol. **183**, 397–404 (2018).

4. Prasannalakshmi, P. & Shanmugam, N. Fabrication of TiO_2/ZnO nanocomposites for solar energy driven photocatalysis. *Mater. Sci. Semicond. Process.* **61**, 114–124 (2017).

5. Bhogaita, M. & Devaprakasam, D. Hybrid photoanode of TiO_2-ZnO synthesized by co-precipitation route for dye-sensitized solar cell using phyllanthus reticulatas pigment sensitizer. *Sol. Energy* **214**, 517–530 (2021).

6. Pugazhendhi, K. *et al.* Plasmonic TiO_2/Al@ZnO nanocomposite-based novel dye-sensitized solar cell with 11.4% power conversion efficiency. *Sol. Energy* **215**, 443–450 (2021).

7. Pawar, P. S. *et al.* Design and photovoltaic studies of W@TiO_2/rGO nanocomposites with polymer gel electrolyte. *New J. Chem.* **47**, 21825–21833 (2023).

8. Pezhooli, N., Rahimi, J., Hasti, F. & Maleki, A. Synthesis and evaluation of composite - TiO_2@ ZnO quantum dots on hybrid nanostructure perovskite solar cell. *Sci. Rep.* 1–9 (2022) doi:10.1038/s41598-022-13903-w.

9. Pawar, P. S. *et al.* nanocomposites with polymer gel electrolyte †. 21825–21833 (2023) doi:10.1039/d3nj04205g.

10. Ako, R. T. *et al.* DSSCs with ZnO@TiO_2 core–shell photoanodes showing improved Voc: Modification of energy gradients and potential barriers with Cd and Mg ion dopants. *Sol. Energy Mater. Sol. Cells* **157**, 18–27 (2016).

11. Marimuthu, T., Anandhan, N., Thangamuthu, R., Mummoorthi, M. & Ravi, G. Graphical abstract SC. *J. Alloys Compd.* (2016) doi:10.1016/j.jallcom.2016.03.219.

12. Zhang, Z., Hu, Y., Qin, F. & Ding, Y. DC sputtering assisted nano-branched core–shell TiO_2/ZnO electrodes for application in dye-sensitized solar cells. *Appl. Surf. Sci.* **376**, 10–15 (2016).

13. Prabakaran, K., Mohanty, S. & Nayak, S. K. Author ' s Accepted Manuscript. *Ceram. Int.* (2015) doi:10.1016/j.ceramint.2015.05.151.

14. Yang, M. *et al.* TiO_2 nanoparticle/nanofiber–ZnO photoanode for the enhancement of the efficiency of dye-sensitized solar cells. *RSC Adv.* **7**, 41738–41744 (2017).

15. Kanimozhi, S., Prabu, K. M., Thambidurai, S. & Suresh, S. Dye-sensitized solar cell performance and photocatalytic activity enhancement using binary zinc oxide-copper oxide nanocomposites prepared via co-precipitation route. *Ceram. Int.* **47**, 30234–30246 (2021).